

RI 9141

RI 9141

Bureau of Mines Report of Investigations/1987

Critical-Load Studies of a Shield Support

By Thomas M. Barczak and David E. Schwemmer

U.S. Bureau of Mines
Spokane Research Center
E. 315 Montgomery Ave.
Spokane, WA 99207
LIBRARY



UNITED STATES DEPARTMENT OF THE INTERIOR



Report of Investigations 9141

Critical-Load Studies of a Shield Support

By Thomas M. Barczak and David E. Schwemmer

UNITED STATES DEPARTMENT OF THE INTERIOR
Donald Paul Hodel, Secretary

BUREAU OF MINES
David S. Brown, Acting Director

Library of Congress Cataloging in Publication Data:

Barczak, Thomas M.
Critical-load studies of a shield support.

(Bureau of Mines report of investigations ; 9141)

Bibliography.

Supt. of Docs. no.: I 28.23:9141.

1. Longwall mining. 2. Mine roof control. I. Schwemmer, David E. II. Title. III. Series:
Report of investigations (United States. Bureau of Mines) ; 9141.

TN23.U43 [TN275]

622 s [622'.334]

87-600280

CONTENTS

Page

Abstract.....	1
Introduction.....	2
Support configuration and load transfer.....	3
Critical-contact configurations.....	5
Support instrumentation and simulator tests.....	8
Results of critical-load tests.....	9
Effect of contact configurations.....	9
Effect of shield height.....	11
Effect of rate of convergence.....	11
Effect of contact stiffness.....	11
Effect of horizontal constraint.....	12
Conclusions.....	12
Appendix A.--Support instrumentation.....	14
Appendix B.--Summary of critical-load test results.....	15

ILLUSTRATIONS

1. Analysis of mine roof support system.....	2
2. Components of longwall shield.....	3
3. Mine roof simulator.....	4
4. Most efficient support-contact configuration.....	4
5. Impact of resultant force acting at locations other than leg reaction....	5
6. Example of critical-load contact configuration.....	5
7. Critical-load canopy contacts.....	6
8. Critical-load base contacts.....	6
9. Canopy-base critical-load contact configurations.....	7
10. One-point base-contact critical-load configuration.....	9
11. Effect of contact-material stiffness on shield strains.....	11
A-1. Locations of strain-gauge instrumentation.....	14

TABLES

1. Comparison of strain distribution for various contact configurations.....	4
2. Effect of shield height on strain profiles.....	11
B-1. Summary of critical-load test results.....	15

UNIT OF MEASURE ABBREVIATIONS USED IN THIS REPORT

in	inch	s	second
in/min	inch per minute	st	short ton
pct	percent		

CRITICAL-LOAD STUDIES OF A SHIELD SUPPORT

By Thomas M. Barczak and David E. Schwemmer²

ABSTRACT

One of the primary goals of Bureau of Mines research is to reduce the cost of coal mining by improving the efficiency of longwall supports. One method of achieving this goal is the optimization of stress distribution within the support structure, resulting in a lower overall weight, more fully stressed shield. However, before stress optimization can be initiated, load conditions must be defined that cause maximum stress in the various support components. A finite-element model of a longwall shield was used to identify these critical load conditions. These load conditions were then evaluated in the Bureau's mine roof simulator (MRS) by instrumentation of a longwall shield and measurement of strains in each of the shield components. The critical (canopy-base contact) load conditions were identified that can cause structural failure at less than rated shield (hydraulic yield) capacity. Comparisons were made between full-contact and partial-contact load conditions. Other parameters investigated included the stiffness of the contact material, changes in shield geometry, rate of load application, and effects of horizontal constraint. Conclusions were drawn regarding the structural integrity of the major shield components and potential for stress optimization.

¹Physicist, Pittsburgh Research Center, Bureau of Mines, Pittsburgh, PA.

²Structural engineer, Boeing Services International, Pittsburgh, PA.

INTRODUCTION

One of the primary goals of the Bureau is to reduce the cost of coal mining by improving the efficiency of longwall roof supports. This can be achieved in one of two ways: (1) better selection of roof supports to minimize the utilization of higher-than-needed support capacity, or (2) improved designs providing more efficient load transfer by optimization of stress distributions within the support structure. An overview of the Bureau of Mine's technical approach for the longwall roof support research program is shown in figure 1.

Improvements in selection criteria require a better understanding of the geomechanics of strata control and the interaction of the support with the strata. The capacity and structural integrity of a longwall support must be

compatible with the maximum loading it is expected to sustain underground. Stress optimization can be considered only after the load conditions have been defined that subject each of the support components to maximum loading. This task requires consideration of all possible contact configurations and magnitudes, since accurate load (contact) conditions cannot be predicted from state-of-the-art strata mechanics.

Longwall shields are subjected to numerous contact configurations (load conditions) during their service life; those inducing critical stresses are potentially dangerous to the safety of the miner. Thus a prerequisite to improving support designs is a definition of critical-load conditions. Identification of these critical-load conditions and their impact on support capacity and the structural integrity of the support is the subject of this study.

Most roof support manufacturers conduct physical acceptance tests of longwall supports to verify performance to their design specifications. Most of these tests, however, are intended to verify the hydraulic yield capacity of the support under various load conditions. In general, little emphasis is given to analysis of the structural behavior of the support. The performance tests may include cyclic loading of the structure to determine the expected life of the support, but a study of controlled failure mechanics is not attempted.

Most state-of-the-art longwall supports are designed quite robustly with very high factors of safety to minimize the financial risk associated with inadequate roof support in longwall mining. These structures, while effective, are crude and may be significantly oversized or underutilized. There appears to be little effort by the mining industry to optimize these structures since, for the most part, they are an effective means of strata control. However, as indicated in this research, there are contact configurations that cause yielding of shield components at loads much less than rated shield capacity. Conversely, there is

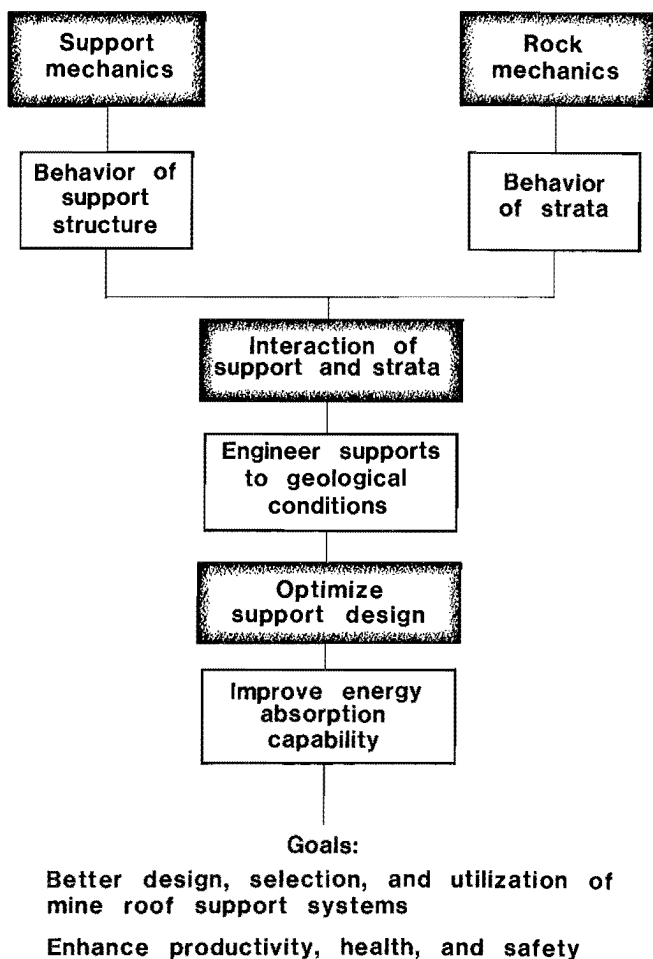


FIGURE 1.—Analysis of mine roof support system.

some evidence to suggest that other components will never experience yield. Thus the motivation for optimization is to provide a more uniformly stressed design and, in the process, reduce the cost and improve the efficiency of the support.

SUPPORT CONFIGURATION AND LOAD TRANSFER

The basic structural components of a typical longwall shield (fig. 2) include (1) canopy, (2) caving shield, (3) lemniscate links, and (4) base. The components are interconnected by hinge pins and hydraulic cylinders. Each component is subjected to bending, axial, shear, and torsional loading to some degree owing to the activity of the strata and mechanics of load transfer within the shield. Analysis of the various canopy-base support configurations suggests possible mechanics for load transfer and conditions for maximum loading of the various components, which are described as follows:

Canopy

The canopy can be thought to act as a cantilevered beam supported at the leg reaction and canopy hinge pin and is subject to bending from resultant forces acting at locations between the leg reaction and the canopy tip. Stiffness properties and configurations of the strata (contact conditions) affect the actual moment distribution on the canopy. The uniaxial strength of the canopy is generally good for the type of loading experienced.

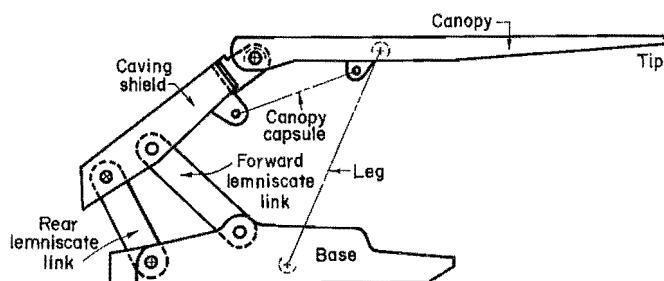


FIGURE 2.—Components of longwall shield.

It is the intent of this research to provide additional insight into the critical loading of longwall supports in preparation for further studies to optimize state-of-the-art longwall support designs.

Caving Shield

The caving shield is subjected primarily to bending stresses due to reactions at the canopy hinge pin and lemniscate links and can also be viewed as a beam under certain contact configurations. Some axial loading also occurs in response to reaction at the canopy hinge pin.

Lemniscate Links

The lemniscate links are primarily subjected to axial loads, with some bending stresses due to pin friction.

Base

The base, like the canopy, is subjected to bending stresses, acting much like a simply supported beam with load transferred from the canopy primarily through the leg cylinder.

The distribution of stresses in the support structure is significantly dependent upon the contact configurations that result from the support and strata interaction. The external work provided by convergence of the strata induces stresses in the various shield components as the shield reacts to strata activity in accordance with the laws of conservation of energy. The primary response of the support is to the displacement (convergence) loading of the roof-and-floor strata. This displacement can be in the roof-to-floor and the face-to-waste direction. While it is recognized that gob loading in the caving shield is not uncommon, contact was restricted to the canopy and base in this study. It is unlikely that gob loading would have any significant impact on stresses in any

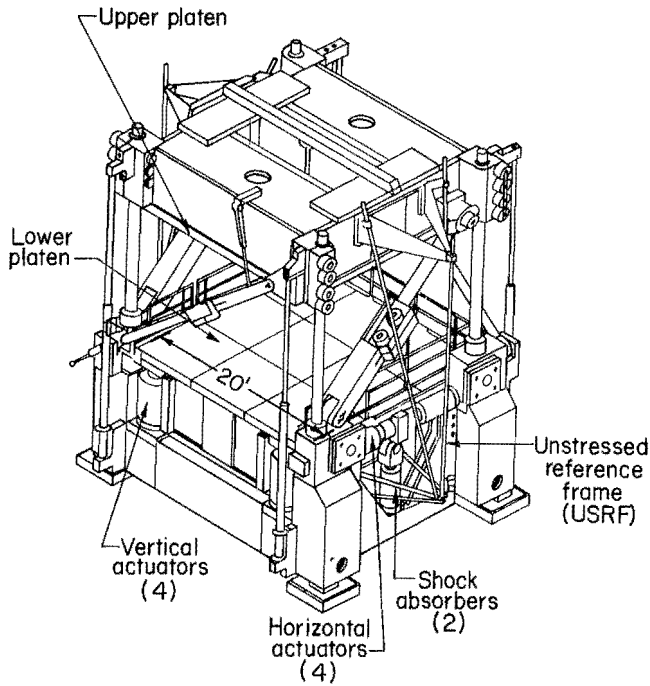


FIGURE 3.—Mine roof simulator.

component other than the caving shield, but further studies are required to quantify the impact of gob loading in the support structure. Since gob loading could not be readily simulated (fig. 3), it was considered beyond the scope of this research. As a percentage of the total external work, gob loading is thought to be less than the displacement loading of the roof and floor strata.

The least stressful shield response, in terms of load transfer and support resistance to roof-to-floor strata convergence, occurs when the actual contact force acts at the location of the leg cylinder on the canopy. One such contact configuration with the base fully supported is illustrated in figure 4. In this configuration, the canopy and base are subjected to very little bending because the load is concentrated at the leg reaction. Since nearly all the roof load is transferred through the leg cylinder to the base, the caving shield and lemniscate links do not undergo much loading, resulting in relatively low stresses in these components. The full-contact base configuration provides an effective distribution of stresses in the

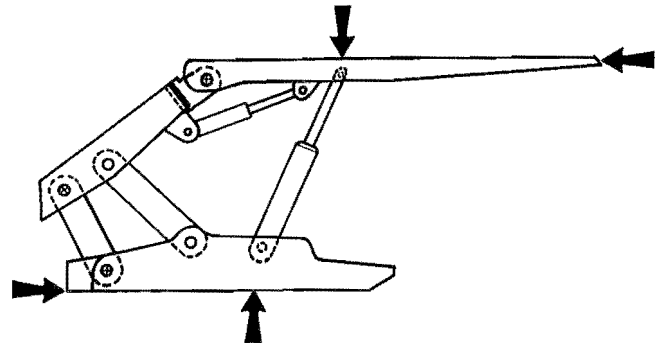


FIGURE 4.—Most efficient support-contact configuration.

base. Measurement taken from strain gauge instrumentation during loading of a shield support in the mine roof simulator with this contact configuration reveals that none of the support components were stressed beyond 39 pct of the material yield, as shown in table 1. Obviously, this is dependent upon instrumentation location, which was placed throughout the shield at nonstress concentrating regions. The instrumentation location was chosen to provide a useful set of nominal strains for analysis. The values in the table represent the maximum strain readings (expressed as a percentage of material yield) for each component. The shield was loaded to its rated capacity (hydraulic leg yield) during this test.

The impact of contact configuration on support capacity can be seen if the resultant roof force is moved from the leg

TABLE 1. - Comparison of strain distribution for various contact configurations, percent

Canopy-contact location	Material yield	
	At leg cylinder ¹	At ends of canopy ²
Canopy.....	33	100
Caving shield....	39	39
Tension link.....	1	9
Compression link.	1	13
Base.....	21	29

¹At rated shield capacity (800 kips vertical load).

²At 50-pct rated shield capacity (400 kips vertical load).

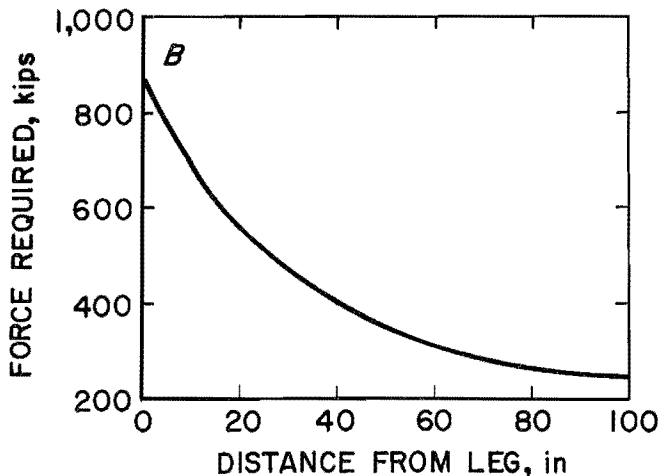
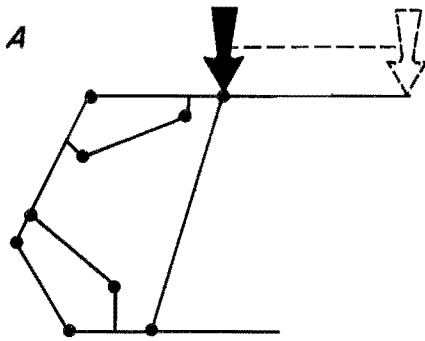


FIGURE 5.—Impact of resultant force acting at locations other than leg reaction. A, Location of resultant force; B, force required to produce leg yield.

reaction toward the canopy tip. Figure 5 shows the roof force required to produce hydraulic yielding of the leg cylinders as a function of the distance of the resultant force from the leg reaction, ignoring canopy stiffness (rigid-body analysis). The change in contact configuration produced by moving the resultant force from the leg reaction also produces a change in the stress distribution within the shield structure.

The change in stress distribution for two contact configurations is seen in

CRITICAL-CONTACT CONFIGURATIONS

The previous section demonstrated the significance of contact configurations on stress distribution within the support structure and provided one example of a critical-load condition where the strength of the support structure

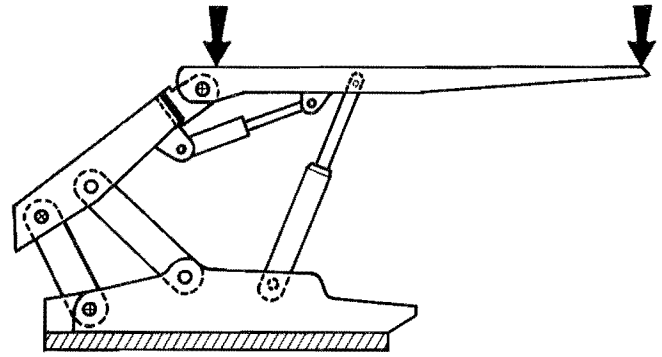


FIGURE 6.—Example of critical-load contact configuration.

table 1, which compares maximum strain readings for the actual contact force coincident with the leg reaction (fig. 4), with the contact configuration illustrated in figure 6. When the load was applied at opposite ends of the canopy, higher stresses occurred in each of the shield components, as illustrated in table 1, at 50 pct of the total load when the load was applied at the leg reaction. The largest increase in stress occurred in the canopy due to additional bending as the load was applied away from the leg reaction. Data show that the strain in the canopy (location A-1, appendix A) approached the yield strength of the steel at less than 50 pct rated shield capacity (hydraulic yield load) for this contact configuration. Therefore, the contact configuration illustrated in figure 6, where the load is applied at opposite ends of the canopy, is considered a critical-load condition since the strength of the support structure material was exceeded prior to the yield load of the leg cylinders. In other words, the hydraulic yield capability of the support would not have prevented structural damage to the support in this load configuration.

(canopy) was exceeded. The purpose of this study is to identify other such critical load cases.

A finite-element model was used to select contact configurations for subsequent physical evaluation in the mine

roof simulator. A simple, two-dimensional beam-element model was constructed consisting of 23 nodes with 3 degrees of freedom per node and 25 elements. Appropriate geometric properties were computed at each nodal location. Use of the beam element, with an insignificant moment of inertia, was extended to represent the hydraulic leg and canopy capsule; only one element type was required for this model. The tapered unsymmetric beam element allowed for a variation in area and moment of inertia between nodes and permitted offsetting the center of gravity of the section from the nodal location.

CANOPY CONTACTS

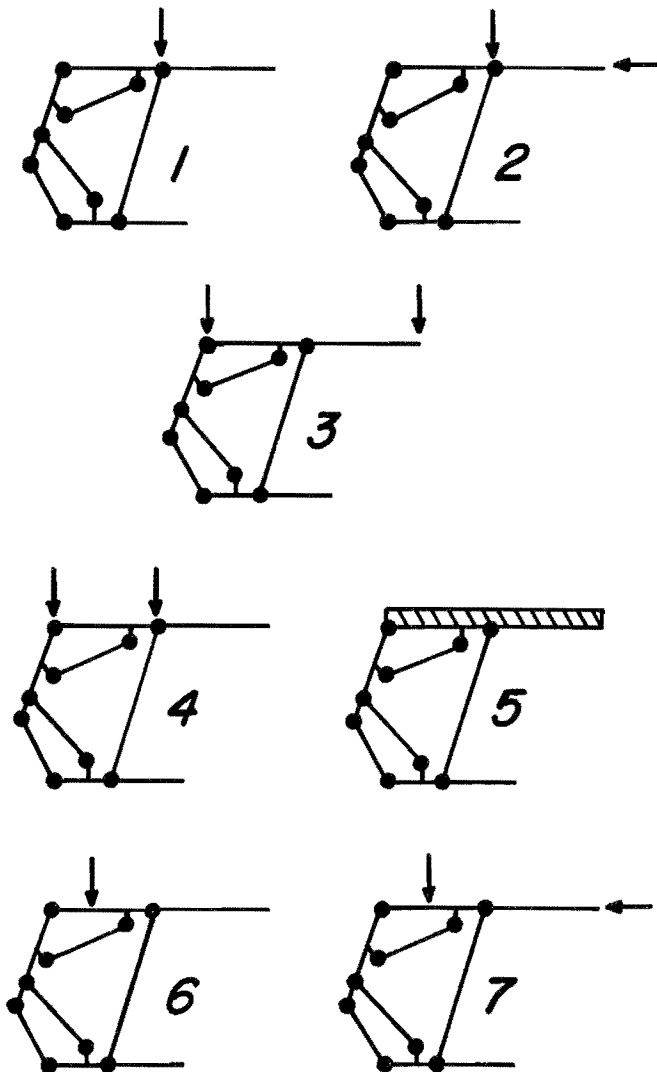


FIGURE 7.—Critical-load canopy contacts.

Linear axial and cubic bending displacements, inherent in the shape functions of this element, are felt to represent the behavior of the shield under typical contact configurations.

Utilizing the finite-element model as a guide, with maximum strain as the governing failure criteria, four base and seven contact configurations were selected for subsequent critical-load evaluations in the mine roof simulator. Figure 7 depicts the seven canopy contacts, and four base contacts are illustrated in figure 8. The combinations of these base and canopy contacts are depicted in matrix format in figure 9. Future references to specific contact configurations will be made from figure 9 using conventional matrix nomenclature, where columns are numbered horizontally and rows vertically. For example, the contact configuration depicted in figure 5 is referenced as (3,2) in figure 9.

The finite-element model utilized to select these contact (load) conditions was relatively simple. Its intent was only to provide general trends concerning load transfer among shield components. It was of insufficient detail to provide an accurate representation of strain profiles in specific shield components. As such, no attempt was made to verify the

BASE CONTACTS

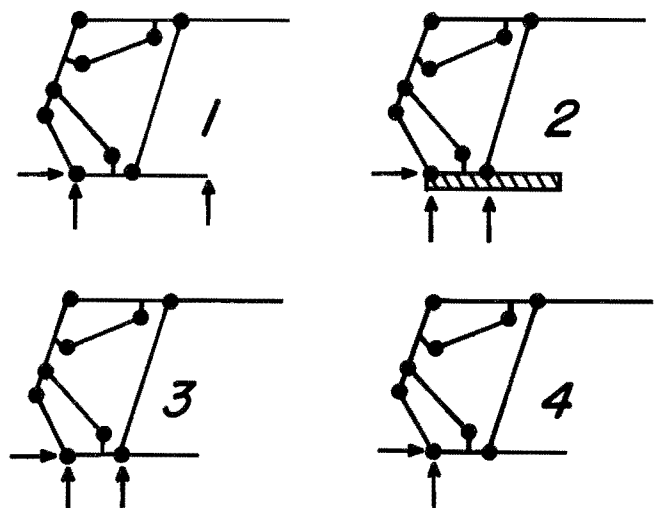


FIGURE 8.—Critical-load base contacts.

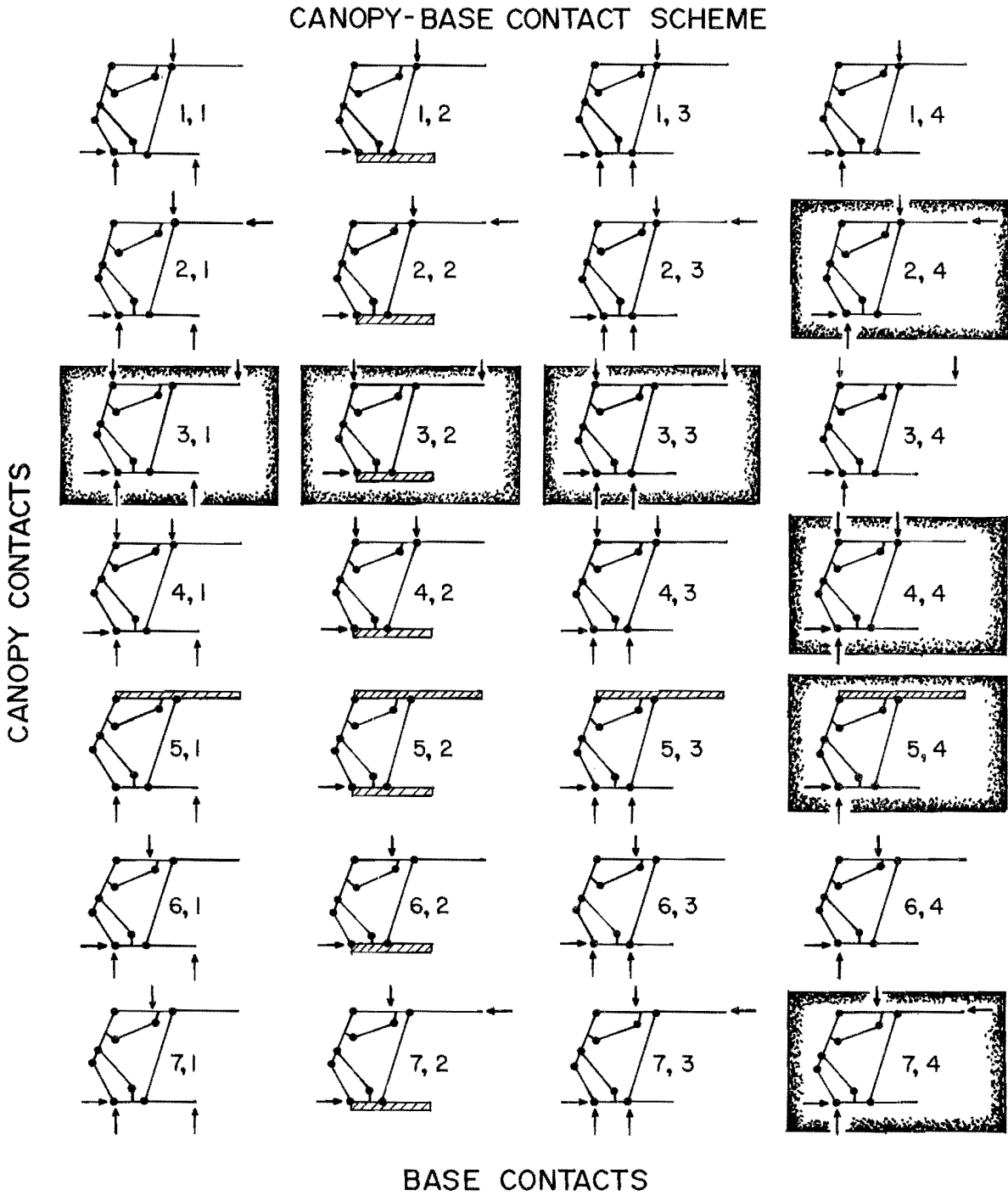


FIGURE 9.—Canopy-base critical-load contact configurations.

the model with test results; however, the general behavior of the shield as

observed during the tests was consistent with the model predictions.

SUPPORT INSTRUMENTATION AND SIMULATOR TESTS

A two-legged shield support of 400-st capacity was instrumented with 72 strain gauges to measure the strain in each of the shield components. Placement of the strain gauges coincided approximately with nodal locations of the finite-element model. The specific locations of the strain gauges on each shield component are identified in appendix A.

The instrumented support was tested in the Bureau's mine roof simulator (MRS) under the contact configurations illustrated in figure 9. These test configurations required the application of vertical load to the support specimen as well as horizontal restraint of the support structure to generate a horizontal load reaction. The simulator generated shield load by controlled vertical displacement of the support structure at a 0.1 in per min rate. Convergence was halted just prior to the hydraulic yield of the leg cylinders (850 to 900 kips vertical load), or when 85 pct of material yield (approximately 1,200 microstrains) was recorded on one or more of the strain gauges. Tests were also terminated if the horizontal support reactions generated exceeded the 300- to 350-kip capacity of the horizontal support fixture. Strain gauge instrumentation, MRS vertical and horizontal load, and vertical displacement were monitored during each test. Data from the specimen strain gauges and the MRS were recorded every 2 s. Strain profiles were developed for each shield component. Maximum strain readings were recorded and computed as a percentage of material yield to evaluate the structural integrity of the support.

The parameters that were thought to influence strain profiles or stress distribution were incorporated in the testing program; these included the following:

1. Shield height. - The geometry of the support structure changes as a

function of height, which changes the load transfer in the shield structure. To evaluate the effect of change in support geometry on the stress distribution, two shield heights, 87.5 in and 65.0 in, were selected for testing. Both test heights are considered to be within the operating range of the support and are common in longwall mining.

2. Rate of convergence. - The rate of convergence may also have an impact on the distribution of stresses within the support structure. Two points of concern are discussed. First, from the principles of fracture mechanics, it is known that the critical-stress intensity factor decreases in metals for increasing load rate. This means that the material will fail at a smaller load, or higher stresses will occur at points of high stress concentration at the same load as the rate of loading increases. Second, there may also be some load rate effects due to friction in the support structure (pin points) or other mechanical considerations that may alter the load transfer. Two convergence rates, 0.1 in/min and 1.0 in/min, were evaluated in these tests.

3. Contact material stiffness. - The interaction of the support with the strata may also be dependent upon the physical properties of the strata. In particular, the stiffness of the strata may significantly affect the loading of the support under partial contact configurations. Five material contacts were investigated:

Type 1.--Stiff, rough, uneven strata were simulated by solid, 5-in-wide, steel blocks.

Type 2.--Point contact loading of stiff, uneven, frictionless strata was simulated with a 4-in-diameter steel rod.

Type 3.--Stiff, rough, brittle, uneven strata behavior was simulated with 7.5-in-wide, fiber-reinforced concrete blocks (with a compressive strength of approximately 5,000 psi) for shield contact.

Type 4.--Strata low in stiffness and with large deformation capability were simulated with 3.5-in wood blocks.

Type 5.--Competent, even strata were simulated by full contact of the support canopy and base with the steel platens of the MRS.

RESULTS OF CRITICAL-LOAD TESTS

EFFECT OF CONTACT CONFIGURATIONS

The most critical-contact configurations were those with two-point canopy contacts occurring at the opposite ends of the canopy (canopy-contact configuration 3, illustrated in figure 7) and single-point base contacts where the contact occurred away from the leg reaction (base-contact configuration 4, illustrated in figure 8).

Loading the canopy at the tip and at the caving shield joint produces bending stresses in the canopy structure. Tests show that strains in the canopy (at location A1, appendix A) approached the yield strength of the material at vertical loads of less than 50 pct of the rated shield capacity (hydraulic leg yield). The critical bending of the canopy under these contact conditions is largely independent of the base contact for a minimum of two-point base contacts. The reason that two-point base contacts do not strongly influence the canopy strains is that the base is a relatively stiff, flexural section, when compared with the canopy. Therefore, under various two-point base-contact configurations, the leg-bottom reaction is resisted with minimal base strains developed. This behavior translates to the canopy as a stiff contact point (at the top of the leg). Thus, when the actual load of the canopy contact is not coincident with the

4. Effect of horizontal constraint. - The shield support responds with a horizontal load reaction to vertical (roof-to-floor) convergence. If the canopy is unrestrained, the horizontal load is limited by the friction at the canopy-strata interface. If the canopy is restrained (e.g., by striking a step in the roof), additional horizontal loads can be generated. The extent to which horizontal constraint (horizontal load) impacts the strain profiles in the support was evaluated by selecting loadcases with and without horizontal constraint.

leg reaction, bending of the canopy occurs, which induces critical stresses due to the low flexural stiffness of this structural section.

Single-point base contacts, where the contact occurs away from the leg reaction, causes a somewhat unique load transfer in the shield support. Since the caving shield-lemniscate assembly is assumed to have little vertical stiffness, vertical loads acting on the canopy must still be transferred to the base via the leg cylinders. Without a support on the base at the leg reaction, stability of the base must be provided by other means. Stability is provided by the lemniscate links in this single-point contact condition. The mechanics of this situation can be seen by analysis of figure 10.

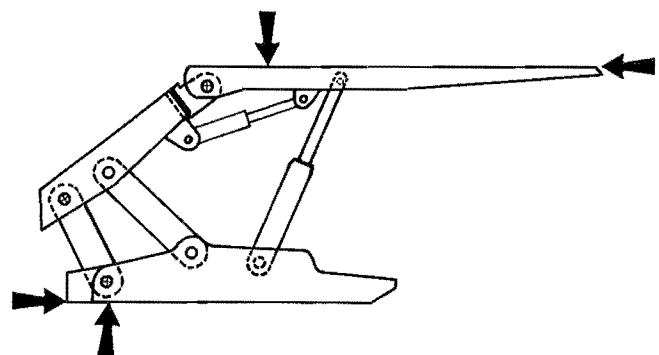


FIGURE 10.—One-point base-contact critical-load configuration.

The load transferred by the leg cylinders to the base tries to rotate the base about the single-point rear contact. Since the caving shield is restrained (from displacement) by reactions developed at the canopy-caving shield hinge pin and the rear link-caving shield hinge pin, the forward lemniscate link can be used to resist this rotation. Considering the caving shield in this situation to act as a beam supported at its ends, the tension force developed in the forward link as it tries to "hold up" the front of the base, induces critical stresses in the caving shield due to bending.

Test results indicate that strains in the caving shield approached material yield at less than 50 pct rated shield capacity (vertical yield load) with horizontal loads of 300 kips acting on the canopy for the single-point base-contact load condition illustrated in figure 9.

The occurrence of single-point base contacts is probably less likely to occur underground than the canopy tip load condition discussed previously. While the single-point base contact is an unlikely occurrence, it is not physically impossible. One scenario for its occurrence would be if the canopy were restrained by striking a step in the roof, and if the rear of the base were resting on a floor step from the previous cut. Under these conditions, the support could be locked in place with the majority of the base being unsupported. As demonstrated in the MRS, this configuration is physically stable if the support is properly constrained.

Figure 9 depicts a total of seven contact configurations from the 28 combinations examined that produced critical loading in one or more of the shield components. Although seven contact configurations produced critical loading, only two loading mechanisms were occurring: (1) bending of the canopy, or (2) bending of the caving shield. In essence, one canopy-contact configuration and one base-contact configuration produced critical loading. Therefore, only 2 of the 11 canopy- and base-contact configurations resulted in critical stresses, and the base-contact configuration is

considered to be an unlikely occurrence. A summary assessment of the loading of each shield component follows. Summary test results for all contact configurations is provided in appendix B.

Canopy

The canopy is the weakest of all shield components. Critical stresses are produced if the actual contact force acts sufficiently away from the leg reaction to produce bending stresses in the cantilevered canopy.

Caving shield

Roof-to-floor strata convergence generally produces very little loading in the caving shield because the majority of the load is transferred from the canopy to the base by the leg cylinders. If the canopy is displaced relative to the base, or load conditions occur that cause load transfer through the caving shield rather than the leg cylinders, the caving shield can be significantly loaded. Under most conditions, the caving shield receives very little loading.

Lemniscate Links

Since the caving shield is generally not heavily stressed, the lemniscate links also are not heavily loaded. In fact, it appears that even when the caving shield is significantly stressed, which occurs with some one-point base-contact configurations, most of the energy is absorbed by the caving shield, and very little stress is developed in the lemniscate links due to their robust size. It appears that the lemniscate links act primarily to provide guidance to the canopy.

Base

The base was found to be the strongest of all shield components, representing a stiff structure more than capable of absorbing the reactions provided to it by the leg cylinders. The worst-case base loading occurred with contact configuration (5,1) (fig. 9), which produced a

TABLE 2. - Effect of shield height on strain profiles (maximum strain)

Shield height.....	Low ¹	High ²
Canopy.....	-550	-650
Base.....	79	90
Caving shield.....	250	305

¹Maximum vertical load acting on canopy = 450 kips.

²Maximum vertical load acting on canopy = 550 kips.

maximum strain of 830 microstrain, or about 60 pct of material yield, at the bottom of the base approximately under the leg (location 3, appendix A).

EFFECT OF SHIELD HEIGHT

Lower shield heights produced mostly lower strains (stresses) in each shield component than did identical canopy-base contacts at a higher shield height. The primary reason for this is the reduced stiffness of the shield with increasing heights, which is largely due to the increased flexibility of the leg cylinders when they are extended at higher shield heights. Since the shield stiffness is less, the same loads will produce larger displacements, resulting in more strain developed at the higher shield heights. The difference in strain readings for the high and low shield heights for the canopy, base, and caving shield for contact conditions (3,1) and (5,2) are shown in table 2.

EFFECT OF RATE OF CONVERGENCE

Limited test results regarding the effect of rate of convergence on strain profiles of the shield structure remain inconclusive. Similar contact configurations were shown to exhibit an apparent rate effect in one contact configuration but not the other. Canopy strains were found to increase by nearly 25 pct for a fast (1.0 in/min) displacement rate as compared with a slow (0.1 in/min) displacement rate for contact (3,1) in figure 9. These observations indicate a reduction in stiffness (by a factor of 2) for the fast loading rate. However, contact configurations (3,2) (fig. 9) with

an identical canopy-contact configuration did not indicate a loading-rate effect. Although the base-contact configuration was different, it is not believed that this accounted for the difference, since other tests indicated the change in base contacts did not significantly alter strain profiles in the canopy. Additional tests are required to determine if there exists a rate effect in the loading of a longwall shield. It should also be recognized that the convergence rate of a longwall face is more likely to be similar to the slow (0.1 in/min) than to the fast (1.0 in/min) rate under normal conditions.

EFFECT OF CONTACT STIFFNESS

As discussed in the section on Support Instrumentation and Simulator Tests, tests were conducted with five contact materials, each with different physical properties, to simulate different strata materials and conditions. The results of these tests indicate that the stiffness of the strata material significantly influences the strains developed in the shield.

For a minimum of two-point base-contact configurations, strains in the base were found to be independent of contact stiffness [contact configurations (2,2) in figure 8]. The canopy strains, however, are significantly affected by some contact materials. As illustrated in figure 11, which is a typical plot of canopy microstrain variation when the vertical displacement is applied and removed at 0.1 in/min, the round steel contact provides a concentrated "line" load across

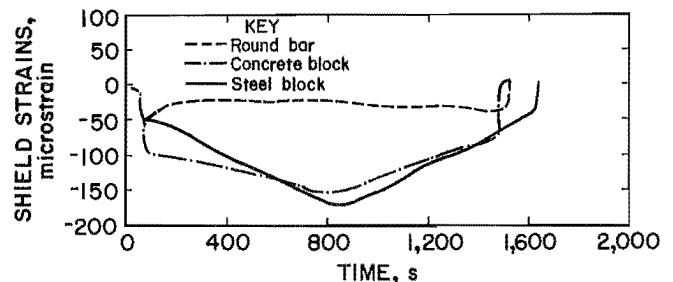


FIGURE 11.—Effect of contact-material stiffness on shield strains.

the canopy width without inducing a "line" bending moment at the point of load application. [The results shown in figure 10 are for gauge location 4, appendix A, for contact configurations (2,2) in figure 8.] The round steel contact resulted in less strain in the canopy in comparison to contact materials that develop a "line" moment, such as those with similar characteristics to the steel and concrete utilized in this study.

One-point base contacts also exhibited a dependency on contact stiffness; however, there did not seem to be a particular contact stiffness that produced consistently larger strains than the others.

EFFECT OF HORIZONTAL CONSTRAINT

The general effect of a restrained canopy tip is to reduce the strains in the base and caving shield and to increase the strain in the canopy. The increase in strain in the canopy may be attributed to the additional stressing of the canopy in the region between the leg reaction and the canopy tip. Previous tests have shown the canopy to have weak bending strength in this region due to its tapered geometry. It was also shown that bending of the canopy occurs for most load conditions where loads are

applied between the leg reaction and canopy tip. Once bending of the canopy occurs, the effect of a horizontal reaction at the canopy tip will be to increase this bending, thus producing additional stresses in this section of the canopy. This effect is enhanced at lower shield heights because the horizontal reaction at the canopy tip is increased in response to larger horizontal components of the leg force.

Horizontal loads due to constrained canopy-tip conditions also reduce the strains in the caving shield. The horizontal component of the leg force produces a reaction at the caving-shield hinge pin, which induces stresses in the caving shield. When horizontal load is applied to the canopy tip, the reaction at the caving-shield pin is reduced since part of the leg force is consumed in equilibrating the horizontal tip force. Therefore, unconstrained canopy-tip conditions increase stresses in the caving shield while constrained canopy-tip conditions generate horizontal loading, which reduces caving-shield loading.

Likewise, base strains are slightly reduced under constrained canopy-tip conditions since caving shield and, therefore, link loads are less. However, since the base has such high flexural stiffness, the effect is small.

CONCLUSIONS

Loading conditions were found to have a significant influence on the distribution of stresses within a longwall shield. In this study, a series of canopy- and base-contact configurations were evaluated to identify those conditions that induced yield strains in the shield at less than rated support capacity. In addition, several parameters, other than contact configuration, which were thought to influence the strain loading of the structure were evaluated.

The results of this critical-load study of shield supports is summarized as follows:

1. Two critical-contact configurations were discovered that produced yield strains at less than 50 pct of rated

shield capacity. These were (1) tip loading of the canopy where the canopy yield strength was exceeded, and (2) single-point base contact at the rear of the base, which approached yield of the caving shield.

2. The base and lemniscate links are very robust; the canopy and caving shield represent the weaker components. Critical loads were never approached in the base and lemniscate links. The canopy is the most likely component to be structurally damaged in a longwall shield.

3. The canopy-contact configuration determines the strain profiles in all components except the base. Base strains are generally independent of the canopy contact owing to the large flexural stiffness of the base component.

4. Higher shield heights generally produce more strain in the support components than do lower shield heights due to reduction in shield stiffness at the higher heights.

5. The effects of rate of loading are not conclusive, but suggestive of (1) a mechanical consideration, or (2) some alteration of the frictional forces in the shield structure affecting the load transfer, and thus the development of stresses.

6. The effects of contact stiffness were significant to the strains developed in the shield, suggesting that the properties and type of strata commonly encountered in a longwall operation should be given consideration in the design of these structures.

7. Effects of horizontal restraint of the canopy tip are significant, and suggest that roof strata conditions, which consist of stiff protrusions, will induce more strain in the canopy than will roof strata with less capacity.

In conclusion, it appears that the efficiency of the shield support can be significantly improved by more efficient distribution of stresses within the

support structure. Under normal load conditions, the shield support is considerably overdesigned. Only the canopy component appears endangered from critical-load conditions. (The critical loading of the caving shield occurs only in a rather unusual load condition.) Hence, it appears the potential exists to reduce the cost and improve the efficiency of the state-of-the-art longwall shield by structural optimization of the components. Optimization could also provide a lighter weight support, which would be beneficial in terms of transportation of these structures in and out of the mine and from face to face.

This study is to be considered a precedent to further studies that refine the distribution of loads in state-of-the-art shield supports. This study was limited to symmetrical load conditions. Unsymmetrical load conditions need to be evaluated before conclusive evidence can be provided regarding the optimization potential of state-of-the-art longwall shields. Additional shield designs must also be evaluated to determine if the trends observed in this study are universal to all shield designs.

APPENDIA A.--SUPPORT INSTRUMENTATION

Figure A-1 illustrates the locations of strain-gauge instrumentation on the shield support.

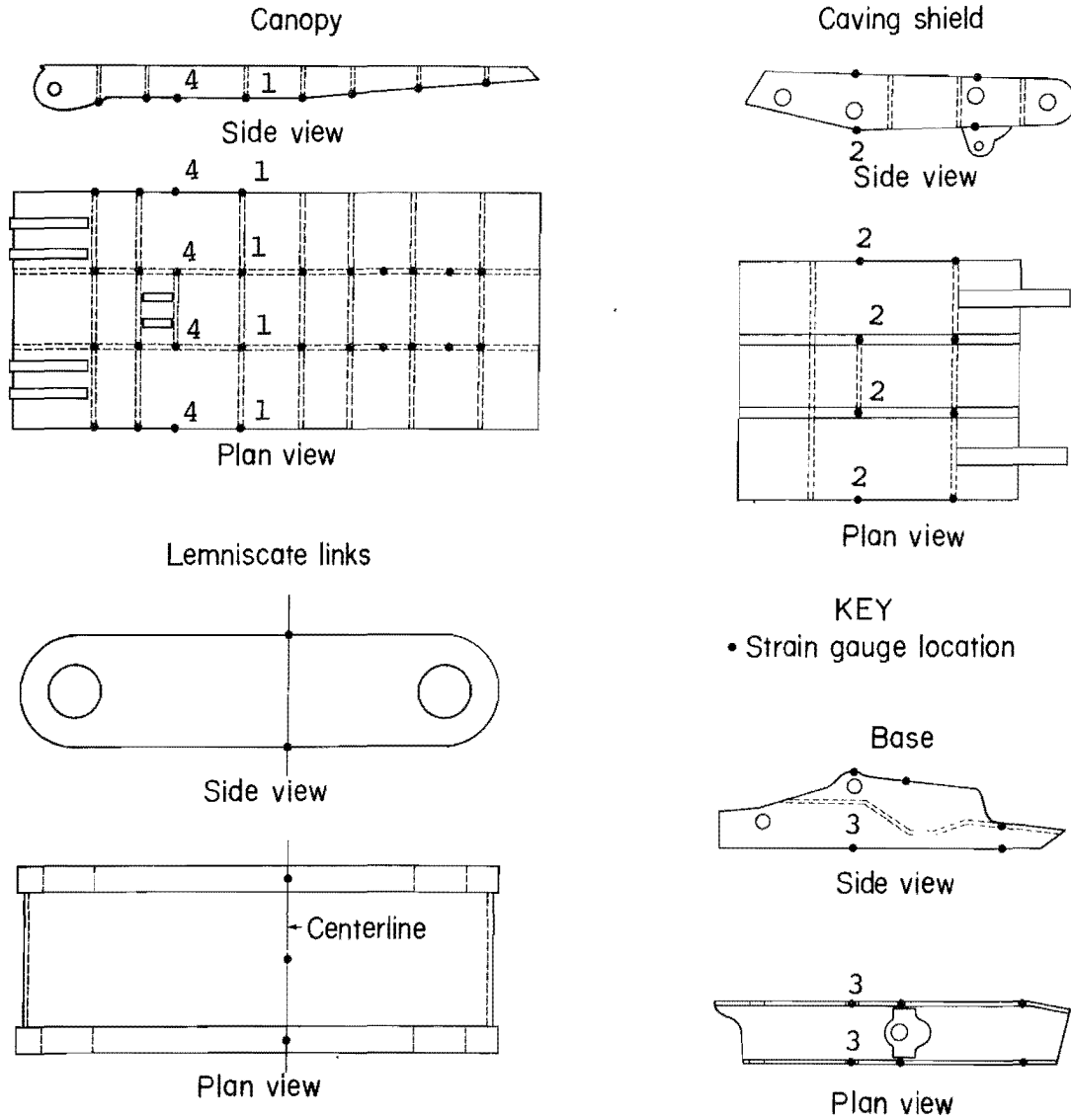


FIGURE A-1.--Locations of strain-gauge instrumentation.

APPENDIX B.--SUMMARY OF CRITICAL-LOAD TEST RESULTS

TABLE B-1. - Maximum strains as percentage of material yield, percent

Test ¹	Canopy	Caving shield	Tension link	Compression link	Base	Note
1, 1.....	-20	25	17	-14	-73	Exceeded rated capacity of shield (800 kips).
1, 2.....	32	29	15	-19	-47	Do.
1, 3.....	63	26	9	-16	-15	Do.
2, 1.....	32	7	8	-11	-62	Do.
2, 2.....	-33	8	1	1	-21	Do.
2, 3.....	-22	39	-8	-15	52	Exceeded 300 kips horizontal fixture capacity.
2, 4.....	17	-29	-17	16	40	Do.
3, 1.....	-100	23	7	-13	-51	Strain exceeded 0.85 of yield strain at a location.
3, 2.....	-100	39	10	-12	-29	Do.
3, 3.....	-76	12	5	-10	4	Configuration was not stable
4, 1.....	53	2	1	-2	-54	Exceeded rated capacity of shield (800 kips).
4, 2.....	-27	9	6	-6	-22	Do.
4, 3.....	-21	-2	2	-2	3	Do.
4, 4.....	-17	63	-18	19	42	Exceeded 300 kips horizontal fixture capacity.
5, 1.....	-42	7	6	-7	58	Exceeded rated capacity of shield (800 kips).
5, 2.....	-53	9	6	-6	-20	Do.
5, 3.....	53	5	6	-6	-10	Do.
5, 4.....	-25	58	-20	21	43	Exceeded 300 kips horizontal fixture capacity.
6, 1.....	-17	42	16	-21	-70	Exceeded rated capacity of shield (800 kips).
6, 2.....	-26	39	10	-15	-31	Configuration was not stable.
6, 3.....	-26	39	10	-15	-31	Do.
7, 1.....	-60	7	2	-3	-55	Exceeded rated capacity of shield (800 kips).
7, 2.....	-83	9	3	-5	-21	Do.
7, 3.....	-36	7	5	-9	5	Configuration was not stable.
7, 4.....	-40	65	-16	20	32	Exceeded 300 kips horizontal fixture capacity.

¹Reference figure 9 of text.